Intrinsic Determinants of Neurotoxic Aggregate Formation by the Amyloid β Peptide

Ann-Christin Brorsson,[†] Benedetta Bolognesi,[†] Gian Gaetano Tartaglia,[†] Sarah L. Shammas,[†] Giorgio Favrin,[†] Ian Watson,[†] David A. Lomas,[‡] Fabrizio Chiti,[¶] Michele Vendruscolo,[†] Christopher M. Dobson,[†] Damian C. Crowther,[§*] and Leila M. Luheshi[†*]

[†]Department of Chemistry and [‡]Department of Medicine, Cambridge Institute for Medical Research, and [§]Department of Genetics, University of Cambridge, Cambridge, United Kingdom; and [¶]Dipartimento di Scienze Biochimiche, Università degli Studi di Firenze, Firenze, Italy

ABSTRACT The extent to which proteins aggregate into distinct structures ranging from prefibrillar oligomers to amyloid fibrils is key to the pathogenesis of many age-related degenerative diseases. We describe here for the Alzheimer's disease-related amyloid β peptide (Aβ) an investigation of the sequence-based determinants of the balance between the formation of prefibrillar aggregates and amyloid fibrils. We show that by introducing single-point mutations, it is possible to convert the normally harmless Aβ_{40} peptide into a pathogenic species by increasing its relative propensity to form prefibrillar but not fibrillar aggregates, and, conversely, to abolish the pathogenicity of the highly neurotoxic E22G Aβ_{42} peptide by reducing its relative propensity to form prefibrillar species rather than mature fibrillar ones. This observation can be rationalized by the demonstration that whereas regions of the sequence of high aggregation propensity dominate the overall tendency to aggregate, regions with low intrinsic aggregation propensities exert significant control over the balance of the prefibrillar and fibrillar species formed, and therefore play a major role in determining the neurotoxicity of the Aβ peptide.

INTRODUCTION

In addition to their familiar compact and frequently highly intricate native folds, proteins can adopt a second, highly ordered conformation, the amyloid fibril, whose core structure is an array of β-strands oriented perpendicular to the fibril axis (1). This alternative structure is frequently stable over a range of solution conditions, and its formation appears to be a consequence of the intrinsic character of the polypeptide backbone (2,3). Although the ability to form amyloid fibrils is a generic property shared by many, if not all, peptides and proteins, the propensity to aggregate in this way can vary dramatically from one to another, and is determined by the physicochemical properties of the amino acid side chains that are present in a given sequence (4). Indeed, it is possible to use these physicochemical properties to predict the propensity of given polypeptide sequences to aggregate, even under conditions where they normally adopt three-dimensional folds (5,6).

Although there is increasing evidence that amyloid structures have a functional role in a variety of organisms (7), the formation of misfolded amyloid fibrils in humans appears at present to be primarily associated with disease states. These include many of the most common and most devastating neurodegenerative disorders, such as Alzheimer's disease (AD), Parkinson's disease, and Huntington's disease. The detailed pathogenesis of these diseases is not yet fully defined, but there is increasing evidence that the oligomeric prefibrillar precursors of amyloid fibrils may in fact be highly toxic, whereas the fibrils themselves are likely to be relatively harmless and their formation could indeed be protective in some cases (8–10).

One of the most intensively investigated amyloid-associated neurodegenerative disorders is AD. In this condition, fibrils consisting of the amyloid β (Aβ) peptide are deposited in extracellular plaques in the cortex of the brain. Many studies, however, have shown that such plaques can also be present in the absence of clinical signs of dementia (11,12), and that the extent of plaque formation correlates only poorly with cognitive dysfunction in animal models of Aβ (13). Recent studies have instead implicated a variety of aggregated forms of Aβ as causes of cognitive dysfunction and neurodegeneration in AD. These range in size from dimers to much larger soluble oligomers (13,14), which are known to be populated before fibril formation occurs. Because of their likely role in pathogenesis, it is important to understand how the intrinsic properties of peptides and proteins such as Aβ determine their relative propensities to form these differentially toxic types of aggregates.

To elucidate the relationship between Aβ aggregation and neurodegeneration, in a previous study we performed a systematic analysis using site-specific mutagenesis of Aβ neurotoxicity in a *Drosophila* model of AD (15). Our strategy is to rationally design mutations using an algorithm that can identify the effects of such mutations on the propensity of Aβ to aggregate into fibrils or prefibrillar aggregates. Using this approach, we identified several mutations that profoundly alter the neurotoxicity of Aβ in vivo but are not, on the basis of our predictions, expected to significantly

Submitted October 27, 2009, and accepted for publication December 23, 2009.

*Correspondence: lml25@cam.ac.uk or dcc26@cam.ac.uk

Ann-Christin Brorsson's present address is Division of Molecular Biotechnology, Department of Physics, Chemistry and Biology, Linköping University, Linköping, Sweden.

Editor: Heinrich Roder.

0006-3495/10/04/1677/8 $2.00

doi: 10.1016/j.bpj.2009.12.4320

influence its propensity to aggregate into fibrils. We suggested, however, that such differences in neurotoxicity could be attributable to changes in the computationally determined propensities of these mutant Aβ peptides to form the moretoxic prefibrillar aggregates before the formation of the potentially benign fibrils. In the study presented here, we set out to test this hypothesis experimentally by undertaking a kinetic and morphological comparison of the in vitro aggregation of two pairs of peptides. Although each pair differs by only a single amino acid, and they have very similar predicted propensities to form β-sheet-rich amyloid, they have also been found to have dramatically different neurodegenerative effects in a *Drosophila* model of AD. The results reveal that the single-point mutations concerned do indeed substantially alter the propensity of Aβ to form prefibrillar aggregates in vitro, strongly supporting the hypothesis that it is these species that give rise to the neuronal degeneration observed in vivo. Furthermore, we show that we can rationalize these effects by examining the biophysical and physicochemical properties of the various mutant Aβ peptides, and gain new insights into the specific determinants of prefibrillar and fibrillar aggregate formation.

MATERIALS AND METHODS

Preparation of the Aβ peptides

The Aβ peptides Aβ_{40}, Aβ_{42}, E22G Aβ_{42}, I31E/E22G Aβ_{42}, and E3R Aβ_{40} were purchased from Bachem (Weil am Rhein, Germany) dissolved in trifluoroacetic acid, and sonicated for 30 s on ice. The trifluoroacetic acid was removed by lyophilization, and the peptides were then dissolved in 1,1,1,3,3,3-hexafluoro-2-propanol and divided into aliquots that were dried by rotary evaporation at room temperature. The amount of peptide in the individual aliquots was determined by quantitative amino acid analysis.

Thioflavin T fluorescence measurement

The peptides were dissolved at a concentration of 30 μM in 50 mM NaH_2PO_4 (pH 7.4) and incubated at 29°C with continuous agitation at 1000 rpm. At regular time intervals, 5 μL aliquots of the peptide solution were removed and added to 100 μL of 20 μM thioflavin T (ThT) in 50 mM Gly-NaOH (pH 8.5). Fluorescence intensity was measured using an excitation wavelength of 440 nm and an emission wavelength of 480 nm on a BMG FLUOstar OPTIMA fluorimeter (BMG Labtech, Aylesbury, UK). The rate of aggregation (k) in each case was determined by fitting the growth phase of fluorescence intensity as a function of time to a single exponential function: $y = q + Ae^{(-kt)}$. Each kinetic experiment was repeated three to five times, and the traces shown in the figures are from a representative experiment.

Size exclusion chromatography

Size exclusion chromatography (SEC) was carried out using an AKTAexplorer (GE Healthcare, Little Chalfont, UK) with a Superdex 200 5/150 GL column (GE Healthcare) operated at 4°C with 0.6% Tween-20 in phosphate-buffered saline (PBS) flowing at 0.3 mL/min. The peptides that eluted from the column were detected by monitoring changes in absorption intensity at 214 nm. The Aβ peptides were initially dissolved in 10 mM NaOH at a concentration of ~1 mg/mL, sonicated for 5 min, and stored at −80°C until required. Peptide solutions were diluted to a concentration of 30 μM in 50 mM PBS buffer, and then diluted with 2.4% Tween-20 in 50 mM PBS to a final concentration of 0.6% Tween-20. Diluted solutions were vortexed for 5 s to generate thorough mixing, and 40 μL aliquots were loaded onto the column immediately. Five replicate chromatograms were collected for each peptide, and background effects were corrected for by subtracting the chromatogram of 0.6% Tween-20 in PBS. The amount of peptide in each peak was determined by measuring the peak areas in the chromatogram using the calculated extinction coefficient of Aβ_{42} of 92,800 $M^{-1}cm^{-1}$ at 214 nm.

Transmission electron microscopy

For transmission electron microscopy (TEM), the peptides were dissolved at a concentration of 30 μM in 50 mM NaH_2PO_4 (pH 7.4) and incubated at 25°C without any agitation beyond that needed for initial mixing. Samples were applied to formvar/carbon-coated copper grids, stained with 2% (w/v) uranyl acetate, and viewed in a Philips CEM100 transmission electron microscope.

Generation of transgenic fruit flies

Mutant Aβ_{42} expression constructs were produced by site-directed mutagenesis of the wild-type (WT) Aβ_{42} sequence in the pMT vector (Invitrogen, Paisley, UK) and subcloned into the pUAST vector. Transgenic fruit flies expressing the desired Aβ_{42} variants were generated according to the procedures described by Crowther et al. (16).

Survival assays

Survival assays were carried out as described previously (15). Survival curves were calculated using Kaplan-Meier plots, and differences between the curves were analyzed using the log rank method. For previously characterized transgenic lines expressing Aβ_{40}, Aβ_{42}, or E22G Aβ_{42}, the survival of one representative line was measured. For the novel mutational variants E3R Aβ_{40} and I31E/E22G Aβ_{42}, six independent lines were analyzed ($n = 100$ for each line) to control for variability in expression levels between individual lines due to the varying location of transgene insertion. The relative reductions in median survival for Aβ transgenic flies (S_{tox}) were calculated relative to Aβ_{40} transgenic flies as S_{tox} = (median survival Aβ_{40} − median survival Aβ_{mut})/median survival Aβ_{40}.

Calculation of aggregation propensities

The propensity to form β-sheet-rich amyloid aggregates (Z_{agg}) was calculated as described previously (5). Briefly, for a given protein, Z_{agg} was obtained by averaging the propensities that were above zero in the aggregation profile of the sequence. All of the propensities were then normalized to generate a variable with an average value of zero and a standard deviation of 1.0 (the normalization is made by calculating the propensities of a set of random sequences). An aggregation profile can contain residues with a propensity larger than 1.0, but these cases are usually sparse and their contribution is diluted upon averaging over the sequence. Consequently, sequences with an overall Z_{agg} score larger than 1.0 are very rare. To calculate the propensity for forming prefibrillar aggregates (Z_{pf}), we used an approach (15) based on an equation containing the same physicochemical contributions used to calculate Z_{agg}, but with specific weights determined using a set of experimentally determined prefibrillar aggregation rates for the protein acylphosphatase (18). A Web server for calculating Z_{agg} and Z_{pf} is available at http://www-vendruscolo.ch.cam.ac.uk/zyggregator.php.

RESULTS

Characterization of mutations that inhibit the toxicity of E22G Aβ_{42} and enhance the toxicity of Aβ_{40} in *Drosophila*

The E22G mutation in Aβ_{42} is associated with an inherited, early-onset form of AD (19). E22G Aβ_{42} is highly

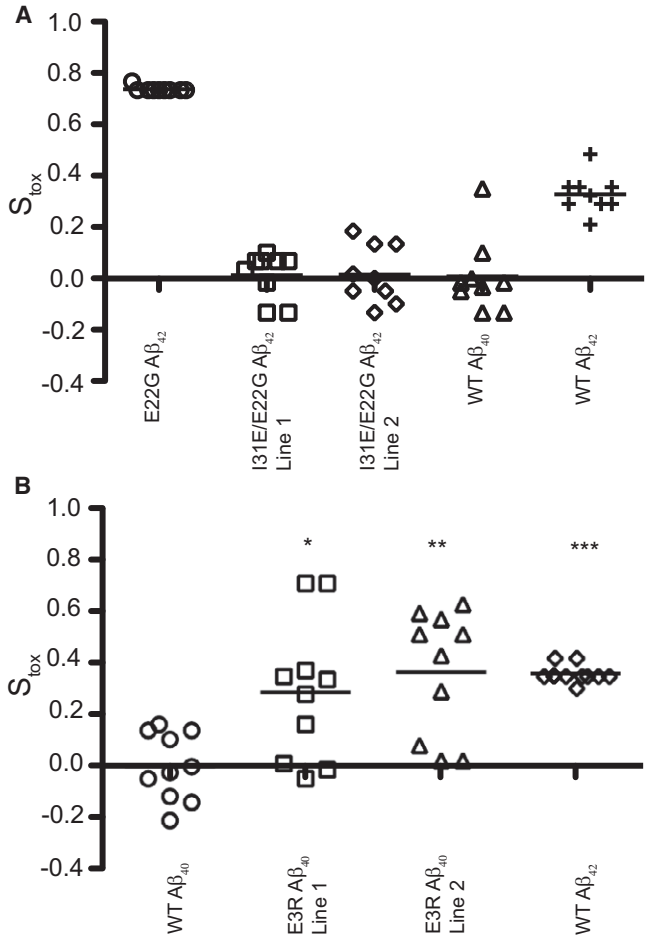

FIGURE 1 Measuring the neurotoxicity of Aβ mutants by their effect on fly longevity. (*A*) The average neurotoxicity (S_{tox}) of a single line of flies expressing E22G Aβ_{42} (○) compared with that of two independent lines of flies expressing I31E/E22G Aβ_{42} (□ and ◇), one line of WT Aβ_{40} (Δ), and one line of WT Aβ_{42} (+). (*B*) The average neurotoxicity of a single line of flies expressing WT Aβ_{40} (○) or WT Aβ_{42} (◇) compared with those of two independent lines of flies expressing E3R Aβ_{40} (□ and Δ); 100 flies divided equally into 10 tubes were analyzed for each line. S_{tox} for each tube ($n = 10$ flies per tube) was calculated from the median survival determined by Kaplan-Meier survival analysis (see Materials and Methods). Differences between lines ($n = 10$ tubes) were analyzed for significance using the Mann Whitney U-test (*$p < 0.05$, **$p < 0.01$, and ***$p < 0.001$).

aggregation-prone in vitro, and its expression in the central nervous system of *D. melanogaster* results in severe neurodegeneration manifested by a 74% reduction in longevity ($S_{tox} = 0.74 \pm 0.01$; see Materials and Methods for the definition of S_{tox}; Fig. 1 *a* (20)) compared to flies expressing the nontoxic Aβ_{40} peptide ($S_{tox} = 0.00 \pm 0.01$). In an earlier study (15), we identified a single-point mutant of E22G Aβ_{42} (I31E/E22G Aβ_{42}) that, in stark contrast, resulted in no significant signs of neurodegeneration when expressed in two independent lines of *Drosophila* (I31E/E22G Aβ_{42} $S_{tox} = 0.01 \pm 0.03$ for line 1, $S_{tox} = 0.01 \pm 0.04$ for line 2; Fig. 1 *a*); indeed, their behavior was indistinguishable from that of flies expressing Aβ_{40}. This result was reproduced in four other independent lines of *D. melanogaster* expressing I31E/E22G Aβ_{42} (15).

Given that this single-point mutation is able to effectively abolish the neurotoxicity of E22G Aβ_{42}, we hypothesized that it must also be possible to convert the Aβ_{40} peptide, which is much less prone to aggregate than E22G Aβ_{42} (or indeed WT Aβ_{42} itself) and is normally harmless in our *Drosophila* model, into a neurotoxic peptide through the alteration of a single amino acid. While investigating a number of single-point mutants of Aβ_{40}, we found that the E3R mutant, when expressed in the central nervous system of two independent lines of *D. melanogaster*, reduced the longevity of the flies by ~30% (S_{tox} E3R A$\beta_{40} = 0.29 \pm 0.08$ for line 1 and 0.37 ± 0.08 for line 2) as compared to flies expressing the nontoxic Aβ_{40} ($S_{tox} = 0.00 \pm 0.01$; Fig. 1 *b*). Indeed, the E3R mutation renders the Aβ_{40} as damaging to the brain as the WT Aβ_{42} peptide ($S_{tox} = 0.36 \pm 0.01$; Fig. 1 *b*) that is primarily responsible for causing neurodegeneration in the brains of patients with AD. This result was reproduced in four other independent lines of *D. melanogaster* expressing E3R Aβ_{40}, each of which has median survival rates significantly shorter than that of Aβ_{40}-expressing flies.

I31E and E3R mutations do not alter the in vitro ThT binding kinetics of E22G Aβ_{42} and Aβ_{40}

From an analysis of their physicochemical properties, neither the I31E mutant of E22G Aβ_{42} nor the E3R mutant of Aβ_{40} are predicted to significantly alter the propensity of their respective parent peptides to form β-sheet-rich aggregates, as both I31 and E3 are located within regions of the polypeptide chain that have a low aggregation propensity and therefore are not rate-limiting for aggregation (Table 1; see Fig. 5). Moreover, we confirmed that prediction experimentally by monitoring the kinetics of aggregation using a ThT fluorescence assay and TEM (k_{agg} E22G A$\beta_{42} = 0.19 \pm 0.08$ min^{-1} and k_{agg} E22G/I31E A$\beta_{42} = 0.10 \pm 0.02$ min^{-1}; Fig. 2, *a*, *c*, and *d*) (15)).

To determine experimentally whether the E3R Aβ_{40} peptide also aggregates at a rate similar to that of its parent peptide, WT Aβ_{40}, we measured the aggregation rates of these two peptides, again using ex situ ThT fluorescence

TABLE 1 Predicted aggregation propensity scores

	Z_{agg} Score	Z_{pf} Score
E22G Aβ_{42}	1.11	0.65
I31E/E22G Aβ_{42}	1.10	0.51
Aβ_{42}	0.97	0.39
Aβ_{40}	0.94	0.37
E3R Aβ_{40}	0.96	0.41

Z_{agg}: The propensity, calculated from the physicochemical properties of the constituent amino acids, of the peptide to aggregate into amyloid fibrils.
Z_{pf}: The propensity, calculated from the physicochemical properties of the constituent amino acids, of the peptide to form prefibrillar aggregates.
See Materials and Methods for details of how Z_{agg} and Z_{pf} are calculated.

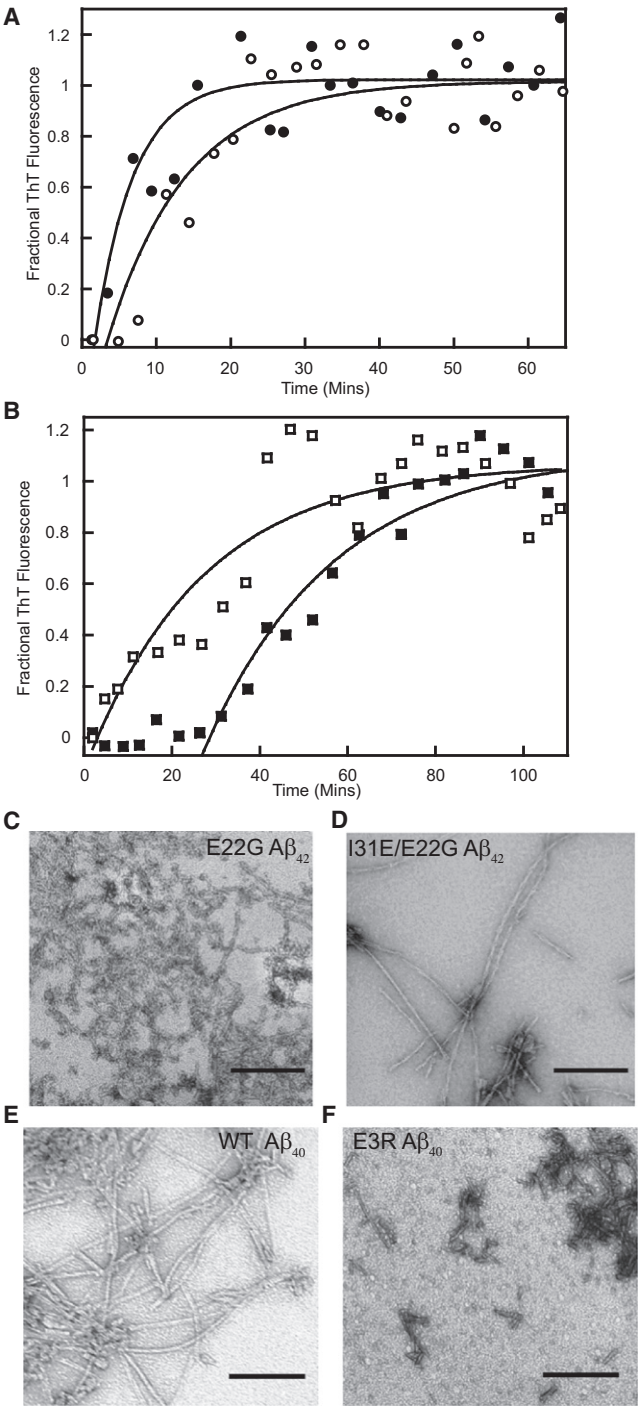

FIGURE 2 Measurement of the kinetics of aggregation and the types of aggregates formed by Aβ_{40}, E22G Aβ_{42}, and their mutants. (*A*) Progression of the aggregation reactions for E22G Aβ_{42} (*solid circles*) and E22G/I31E Aβ_{42} (*open circles*) monitored by ThT fluorescence spectroscopy. (*B*) The progression of the aggregation reactions for Aβ_{40} (*solid squares*) and E3R Aβ_{40} (*open squares*) was monitored by ThT fluorescence spectroscopy. (*C* and *D*) Transmission electron micrographs of samples from the end points of the E22G Aβ_{42} and I31E/E22G Aβ_{42} aggregation reactions shown in *A* indicate that fibrils were formed by both peptides. (*E* and *F*) Transmission electron micrographs of samples from the end points of the Aβ_{40} and E3R Aβ_{40} aggregation reactions shown in *B* indicate that fibrils were formed by both peptides. Scale bar = 200 μm.

and TEM imaging. The E3R Aβ_{40} and WT Aβ_{40} peptides can be seen to aggregate to states that bind ThT and have a fibrillar appearance at very similar overall rates (k_{agg} A$\beta_{40} = 0.034 \pm 0.01$ min^{-1} and k_{agg} E3R A$\beta_{40} = 0.037 \pm 0.01$ min^{-1}; Fig. 2, *b*, *e*, and *f*), again in accord with our predictions (Table 1). The growth of Aβ_{40} aggregates, however, is preceded by a significant lag phase that is notably absent in the aggregation of the E3R Aβ_{40} peptide. This suggests that the early stages of aggregation, unlike the later growth phase, differ significantly for these two peptides under the conditions described here. Of note, the TEM images reveal that larger amounts of prefibrillar species and lower quantities of fibrils are present in the E22G Aβ_{42} and E3R Aβ_{40} samples (Fig. 2, *c* and *f*) relative to their respective counterparts (Fig. 2, *d* and *e*). This is further investigated in the following section.

Effects of the I31E and E3R mutations on the morphology of the aggregates formed by E22G Aβ_{42} and Aβ_{40}

It is well established that Aβ peptides, like other amyloidogenic peptides and proteins, can form a host of prefibrillar aggregates in vitro before the formation of mature amyloid fibrils. These species range in size from dimers to large protofibrillar assemblies visible by TEM in vitro (14,21). Such species have also been detected in transgenic models of AD (13,22) and in postmortem tissue from the brains of patients with AD (14,23). In both cases, the presence of the prefibrillar aggregates has been shown to be correlated with a decline in cognitive function, as well as with defects in long-term potentiation and synaptic loss (24,25). Therefore, it appears possible that the I31E mutation can substantially reduce the neurotoxic properties of E22G Aβ_{42} by altering the balance between its relative propensities to form prefibrillar and mature fibrillar aggregates without significantly altering the overall rate at which the latter are formed.

To investigate this possibility, we monitored and analyzed the morphologies of the aggregates formed by both I31E/E22G Aβ_{42} and E22G Aβ_{42} over the course of their formation. To visualize any oligomers that formed during the course of experiments, both peptides were incubated without agitation to avoid perturbing the nature of the population of such intermediate species. In both cases, no aggregates were detectable by TEM in the solutions examined immediately after dissolution of the monomeric peptides in 50 mM NaH_2PO_4 at pH 7.4 (Fig. 3, *a* and *d*). After 15 min, however, spherical oligomers and short curvilinear prefibrillar aggregates similar to those observed previously with E22G Aβ_{42} (19) were detectable by TEM (Fig. 3 *b*). With I31E/E22GAβ_{42}, however, no such aggregates were observable at the same time (Fig. 3 *e*). The absence of even small aggregates of I31E/E22G Aβ_{42} after 15 min was also confirmed by analysis of the initial preparations of both peptides by SEC

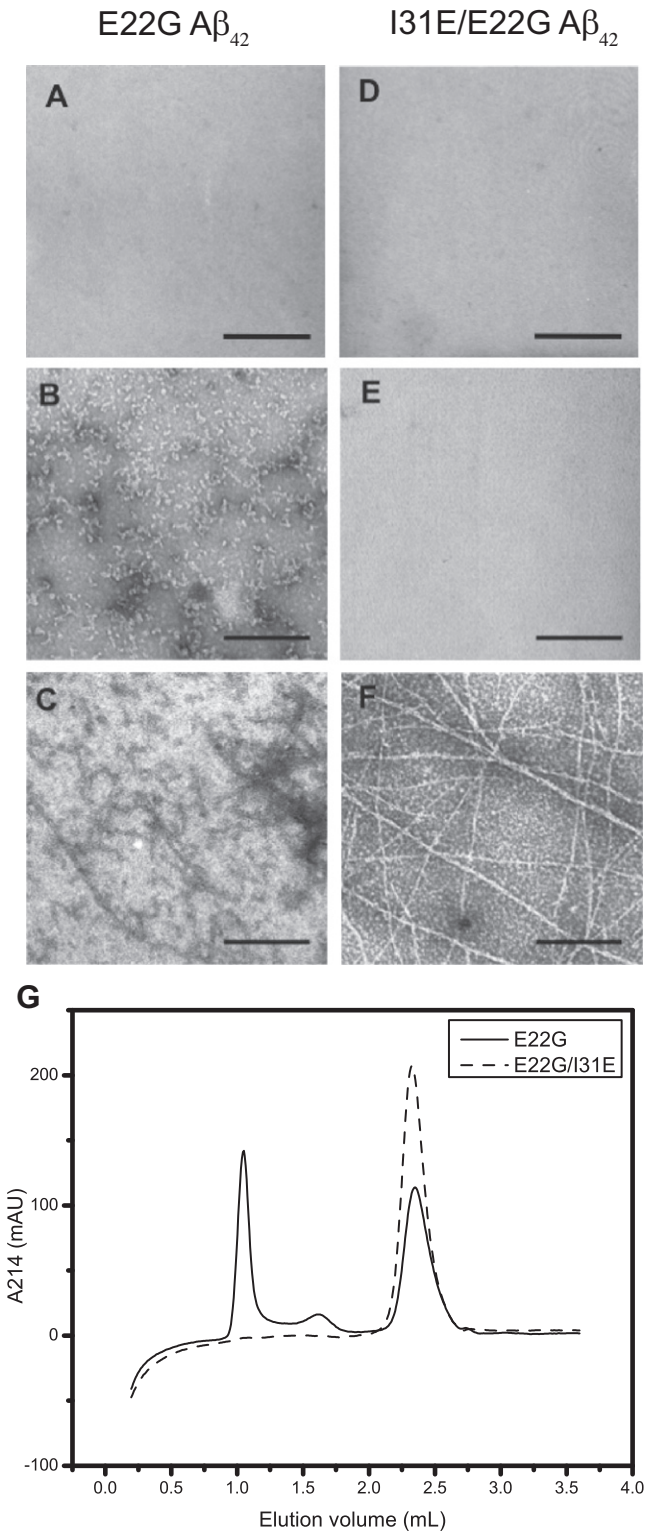

FIGURE 3 Time-course analysis by TEM of the aggregation of E22G Aβ_{42} and I31E/E22G Aβ_{42}. (*A–C*) TEM images taken throughout the aggregation reaction of E22G Aβ_{42} ($t = 0$ min, 15 min, and 6 days, respectively). (*D–F*) TEM images taken throughout the aggregation reaction of I31E/E22G Aβ_{42} (0 min, 15 min, and 6 days, respectively). Scale bar = 200 nm. (*G*) The size distributions of aggregates of E22G Aβ_{42} (*solid line*) and E22G/I31E Aβ_{42} (*dashed line*) determined by SEC performed immediately after dissolution of the peptides.

(see Materials and Methods). Chromatograms of solutions of the E22G Aβ_{42} variant show two distinct peaks—one at a size consistent with low-molecular-weight (LMW) Aβ species (potentially monomer, dimer, and trimer) and another eluting in the void volume—indicating that the solution contained higher-molecular-weight but still soluble aggregate species (Fig. 3 *g*). By contrast, the chromatograms of the solution of I31E/E22G Aβ_{42} at the same time points show only a single LMW peak (Fig. 3 *g*).

Analysis of the E22G Aβ_{42} sample by TEM after 6 days reveals the presence of an abundance of short, curved protofibrillar species and amorphous aggregates accompanied by a small number of well-defined fibrils (Fig. 3 *c*). By contrast, the I31E/E22G Aβ_{42} contains mostly long, straight, mature fibrils (Fig. 3 *f*), and no amorphous or structured prefibrillar assemblies are detectable. These results indicate that the I31E mutation in E22G Aβ_{42} does indeed dramatically reduce the propensity of E22G Aβ_{42} to form prefibrillar species relative to fibrillar species. Provided that such a situation occurs in vivo, this would provide an explanation for the substantially reduced toxicity despite a similar overall aggregation propensity.

To further test this hypothesis, we tested the effect of the E3R mutation on the balance between the population of fibrillar and prefibrillar species in Aβ_{40} through a comparative morphological analysis of the aggregates formed over time in solutions of Aβ_{40} and E3R Aβ_{40}, without agitation, using TEM. In this study no aggregates could be detected for Aβ_{40} after one minute (Fig. 4 *a*) while at the corresponding time point for E3R Aβ_{40} abundant quantities of amorphous aggregates were detected (Fig. 4 *d*). SEC analysis also showed the absence at this early time point of small prefibrillar Aβ_{40} species that are not detectable by TEM (Fig. 4 *g*) as the peptide elutes as a single LMW peak. Surprisingly, considering that prefibrillar aggregates are visible after one minute by TEM, SEC analysis of E3R Aβ_{40} at this time also reveals only a LMW peak, suggesting that the aggregates formed by this variant are relatively unstable and dissociate during separation, or are retained by the column.

After 3 days, long mature fibrils are visible for the Aβ_{40} peptide (Fig. 4 *b*), whereas the E3R Aβ_{40} samples are dominated by large numbers of small globular aggregates (Fig. 4 *e*), with a short fibril being observed very occasionally (Fig. 4 *e*, *inset*). From day 5 onward, fibrils are the dominant species for both peptides, but they have different morphologies. For Aβ_{40} the fibrils are long and very regular (Fig. 4 *c*), whereas the E3R Aβ_{40} fibrils are shorter and significantly irregular in appearance (Fig. 4 *f*). These results indicate that the E3R mutation significantly decreases the relative propensity of the Aβ_{40} peptide to form well-defined and inert fibrillar aggregates. This leads to an enhanced population of oligomeric and other disordered structures, which explains its enhanced toxicity relative to Aβ_{40}.

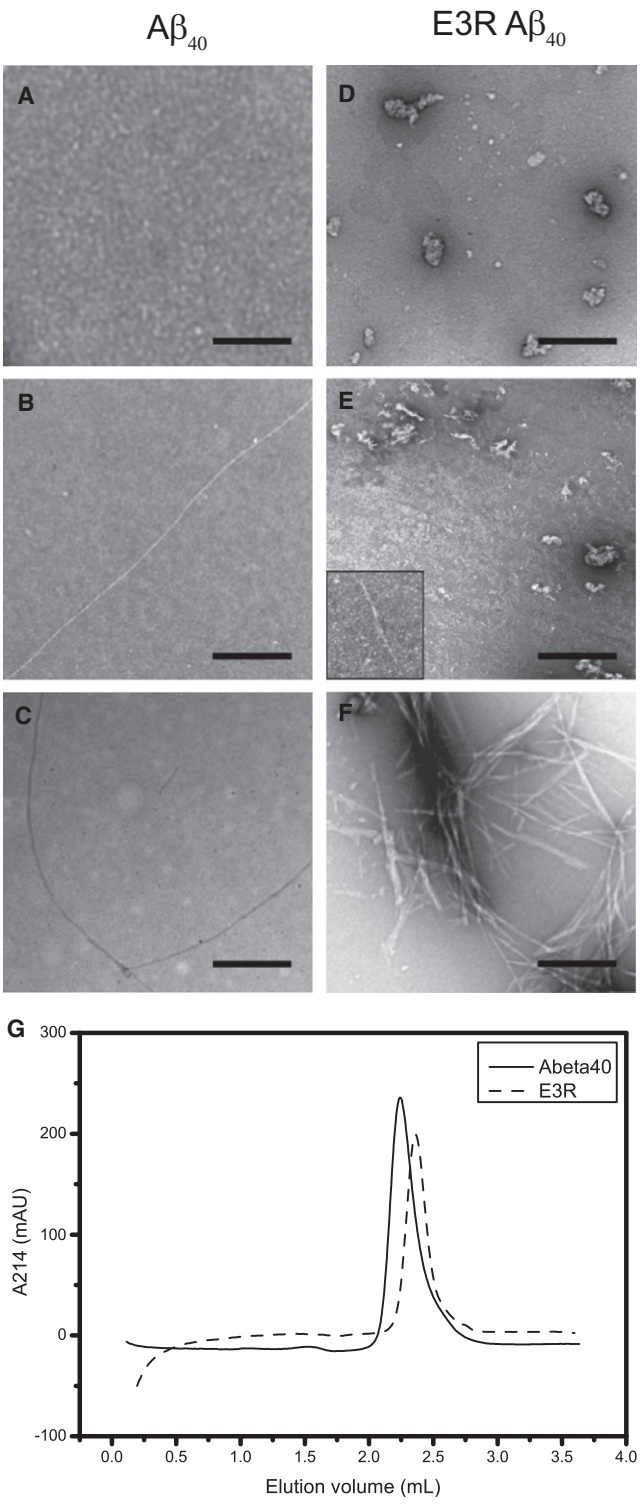

FIGURE 4 Time-course analysis by TEM of the aggregation of Aβ_{40} and E3R Aβ_{40}. (*A–C*) TEM images taken throughout the aggregation reaction for WT Aβ_{40} (1 min, 3 days, and 7 days, respectively). (*D–F*) TEM images taken throughout the aggregation reaction for E3R Aβ_{40} (1 min, 3 days, and 7 days, respectively). Scale bar = 200 nm. (*G*) The size distributions of aggregates of Aβ_{40} peptide (*solid line*) and E3R Aβ_{40} (*dashed line*) determined by SEC performed immediately after dissolution of the peptides.

Rationalization of the relative propensity of peptides and proteins to form prefibrillar aggregates

As we showed in a previous work (6), and further demonstrated here, it is possible to rationalize with a high degree of accuracy the propensity of a given polypeptide sequence to form β-sheet-rich aggregates in vitro (as measured here by ThT fluorescence and TEM) by assessing the intrinsic physicochemical properties of its constituent amino acids. The algorithm (Z_{agg}) we developed for this purpose takes into account the charge, hydrophobicity, and secondary structure propensities of each amino acid, and weights their relative importance using available data from our work and from the literature.

To rationalize the propensity of proteins such as Aβ to specifically form potentially toxic prefibrillar aggregates during the process of amyloid aggregation, we developed a second algorithm based on the same physicochemical properties but parameterized on the basis of aggregation-rate data collected from an extensive study of mutational variants of the muscle acylphosphatase protein (AcP), in which the aggregation process (under the experimental conditions used) culminates specifically in the formation of prefibrillar rather than mature fibrillar assemblies (18). This second algorithm (used previously (15) to generate the parameter Z_{tox}, here renamed Z_{pf}) predicts both that I31E/E22G Aβ_{42} has a lower propensity than E22G Aβ_{42} to form prefibrillar aggregates (Z_{pf} I31E/E22G Aβ_{42} = 0.51; E22G Aβ_{42} = 0.65), and E3R Aβ_{40} has a higher propensity to form prefibrillar aggregates than WT Aβ_{40} (Z_{pf} E3R Aβ_{40} = 0.41; WT Aβ_{40} = 0.37; Table 1).

In this regard, it is particularly striking that the E3R mutation, which renders Aβ_{40} as toxic to the fly brain as the WT Aβ_{42} peptide (Fig. 1 *b*), has a comparable propensity to form prefibrillar aggregates (Z_{pf} Aβ_{42} = 0.39). In summary, therefore, the various predictions for the propensities to form different types of aggregates are consistent with the experimental data presented here, and strongly implicate prefibrillar aggregates as the primary neurotoxic agents, at least in this *Drosophila* model of AD. These findings are highly consistent with those obtained in many other systems indicating that the most highly toxic species associated with amyloid formation are likely to be small aggregates with high surface/volume ratios (26,27).

DISCUSSION

In this study, we investigated two pairs of mutational variants of Aβ: one from the early-onset, disease-related E22G Aβ_{42} peptide, and one from the Aβ_{40} peptide, which is normally harmless in our model system. Each pair was chosen by a rational design strategy to ensure that both members had similar overall propensities to form fibrillar aggregates in vitro but very different neurotoxic properties in vivo in

our *Drosophila* model. We rationalized the different behavior of the two peptides in each of these pairs by identifying significant differences in their relative propensities to form prefibrillar aggregates in vitro during the process of aggregation into mature fibrils. In itself, this study shows that single-point mutations can strongly modulate the aggregation behavior and pathogenic properties of both peptides, a phenomenon that is likely to be generic, i.e., to apply to proteins and peptides generally. In addition, we derived an algorithm that allows us to predict the effect of mutations on both the fibrillar and prefibrillar states of proteins.

A variety of theoretical and experimental observations suggest that aggregation into amyloid fibrils occurs by at least a two-step mechanism in which monomeric polypeptide chains that are either fully or partially unfolded nucleate and condense into relatively disordered prefibrillar oligomeric aggregates, and then reorganize into highly ordered fibrillar structures with a cross-β structure (28,29). In agreement with a range of other studies, this work demonstrates that the morphologies of these two types of aggregates are clearly distinct. It is therefore very likely that the specific nature of the interactions, and the regions of the polypeptide chain that are involved in forming these different structures will differ. Furthermore, it is not surprising that amino acid substitutions can affect different stages of the reaction in a different manner, as we observed in this study, and that the propensities to form these different types of aggregates will differ to some extent. It is particularly useful, therefore, that the algorithms derived from experimental data appear capable of predicting the relative propensities to form the different types of structure, and are robust and potentially widely applicable.

It is particularly interesting in the context of the factors affecting these aggregation propensities that neither of the two mutations discussed here (residues 3 and 31) is located in a region of the Aβ sequence that is predicted to have a high propensity for aggregation (Fig. 5) or has been identified by solution and solid-state NMR studies to be in the core region of the cross-β structure of the Aβ fibril (30,31). This observation is consistent with the finding that neither mutation appears to affect the overall rate of fibril formation (Fig. 2). The fact that both residues do, however, influence the propensity to form prefibrillar aggregates is consistent with the latter being formed through a relatively disordered collapse of the polypeptide chain that must involve a wider range of residues than those that are highly structured in the conformation of the mature fibrils. In support of these observations, we previously found that regions of the amyloidogenic protein AcP, which are not rate-limiting for the formation of protofibrillar aggregates, can nonetheless contribute to their resistance to disaggregation, which again shows that different residues can play a role at different stages of the aggregation process (32). Furthermore, these results enable us to rationalize the recent finding that mutations in the N-terminal region of Aβ are associated with familial AD, in that they can specifically affect the propensity of the peptide to form prefibrillar and potentially neurotoxic aggregates, as previously demonstrated for familial AD mutations, such as E22G, that fall within the highly aggregation-prone hydrophobic core of Aβ (33–35).

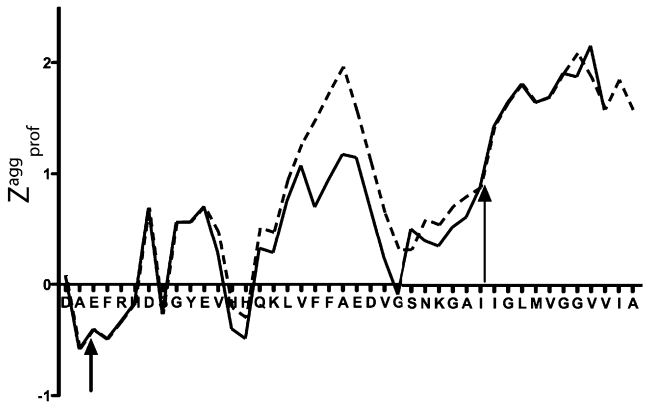

FIGURE 5 Aggregation propensity profiles of Aβ_{40} (*solid line*) and E22G Aβ_{42} (*dashed line*), indicating the locations in negative peaks of the two mutants studied here (E3R Aβ_{40} and I31E/E22G Aβ_{40}).

CONCLUSIONS

We have shown through computational, in vivo, and in vitro studies of mutational variants of the Aβ_{40} and Aβ_{42} peptides that the sequence determinants of the formation of prefibrillar aggregates are related to but distinct from those that control the rate at which a polypeptide chain assembles into amyloid fibrils. The computational methods we used to rationally alter the properties of the Aβ peptides have been shown to be applicable to many different proteins (5); therefore, we propose that these distinctions are likely to be relevant for future investigations of the wide range of proteins that form amyloid fibrils. Furthermore, they may enable us to understand why amyloid aggregation in some cases results in the development of devastating neurological diseases, and in other cases results in the formation of functional, nonpathogenic amyloid fibrils in organisms such as bacteria, yeast, and mammals (36–38).

This work was supported by the Swedish Research Council (A.-C.B.), the Alzheimer's Research Trust (B.M.B.), the Wellcome Trust (C.M.D.), and the Medical Research Council (G.G.T., S.L.S., D.C.C., M.V., C.M.D., D.A.L., and L.M.L.).

REFERENCES

1. Chiti, F., and C. M. Dobson. 2006. Protein misfolding, functional amyloid, and human disease. *Annu. Rev. Biochem.* 75:333–366.
2. Dobson, C. M. 1999. Protein misfolding, evolution and disease. *Trends Biochem. Sci.* 24:329–332.
3. Knowles, T. P., A. W. Fitzpatrick, …, M. E. Welland. 2007. Role of intermolecular forces in defining material properties of protein nanofibrils. *Science*. 318:1900–1903.

4. Chiti, F., M. Stefani, …, C. M. Dobson. 2003. Rationalization of the effects of mutations on peptide and protein aggregation rates. *Nature*. 424:805–808.
5. Tartaglia, G. G., A. P. Pawar, …, M. Vendruscolo. 2008. Prediction of aggregation-prone regions in structured proteins. *J. Mol. Biol.* 380: 425–436.
6. Pawar, A. P., K. F. Dubay, …, C. M. Dobson. 2005. Prediction of ''aggregation-prone'' and ''aggregation-susceptible'' regions in proteins associated with neurodegenerative diseases. *J. Mol. Biol.* 350:379–392.
7. Hammer, N. D., X. Wang, …, M. R. Chapman. 2008. Amyloids: friend or foe? *J. Alzheimers Dis.* 13:407–419.
8. Haass, C., and D. J. Selkoe. 2007. Soluble protein oligomers in neurodegeneration: lessons from the Alzheimer's amyloid β-peptide. *Nat. Rev. Mol. Cell Biol.* 8:101–112.
9. Kayed, R., E. Head, …, C. G. Glabe. 2003. Common structure of soluble amyloid oligomers implies common mechanism of pathogenesis. *Science*. 300:486–489.
10. Karpinar, D. P., M. B. G. Balija, …, M. Zweckstetter. 2009. Pre-fibrillar [α]-synuclein variants with impaired [β]-structure increase neurotoxicity in Parkinson's disease models. *Embo. J.* 28:3256–3268.
11. Neuropathology Group. Medical Research Council Cognitive Function and Aging Study. 2001. Pathological correlates of late-onset dementia in a multicentre, community-based population in England and Wales. Neuropathology Group of the Medical Research Council Cognitive Function and Ageing Study (MRC CFAS). *Lancet.* 357:169–175.
12. Lue, L. F., Y. M. Kuo, …, J. Rogers. 1999. Soluble amyloid β peptide concentration as a predictor of synaptic change in Alzheimer's disease. *Am. J. Pathol.* 155:853–862.
13. Lesné, S., M. T. Koh, …, K. H. Ashe. 2006. A specific amyloid-β protein assembly in the brain impairs memory. *Nature*. 440:352–357.
14. Shankar, G. M., S. Li, …, D. J. Selkoe. 2008. Amyloid-β protein dimers isolated directly from Alzheimer's brains impair synaptic plasticity and memory. *Nat. Med.* 14:837–842.
15. Luheshi, L. M., G. G. Tartaglia, …, D. C. Crowther. 2007. Systematic in vivo analysis of the intrinsic determinants of amyloid β pathogenicity. *PLoS Biol.* 5:e290.
16. Crowther, D. C., R. Page, …, D. A. Lomas. 2006. A *Drosophila* model of Alzheimer's disease. *Methods Enzymol.* 412:234–255.
17. Reference deleted in proof.
18. Chiti, F., N. Taddei, …, C. M. Dobson. 2002. Kinetic partitioning of protein folding and aggregation. *Nat. Struct. Biol.* 9:137–143.
19. Nilsberth, C., A. Westlind-Danielsson, …, L. Lannfelt. 2001. The 'Arctic' APP mutation (E693G) causes Alzheimer's disease by enhanced Aβ protofibril formation. *Nat. Neurosci.* 4:887–893.
20. Crowther, D. C., K. J. Kinghorn, …, D. A. Lomas. 2005. Intraneuronal Aβ, non-amyloid aggregates and neurodegeneration in a *Drosophila* model of Alzheimer's disease. *Neuroscience.* 132:123–135.
21. Walsh, D. M., A. Lomakin, …, D. B. Teplow. 1997. Amyloid β-protein fibrillogenesis. Detection of a protofibrillar intermediate. *J. Biol. Chem.* 272:22364–22372.
22. Oddo, S., A. Caccamo, …, F. M. LaFerla. 2006. Temporal profile of amyloid-β (Aβ) oligomerization in an in vivo model of Alzheimer disease. A link between Aβ and τ pathology. *J. Biol. Chem.* 281:1599–1604.
23. Gong, Y., L. Chang, …, W. L. Klein. 2003. Alzheimer's disease-affected brain: presence of oligomeric A β ligands (ADDLs) suggests a molecular basis for reversible memory loss. *Proc. Natl. Acad. Sci. USA.* 100:10417–10422.
24. Lacor, P. N., M. C. Buniel, …, W. L. Klein. 2007. Aβ oligomer-induced aberrations in synapse composition, shape, and density provide a molecular basis for loss of connectivity in Alzheimer's disease. *J. Neurosci.* 27:796–807.
25. Cleary, J. P., D. M. Walsh, …, K. H. Ashe. 2005. Natural oligomers of the amyloid-β protein specifically disrupt cognitive function. *Nat. Neurosci.* 8:79–84.
26. Volles, M. J., and P. T. Lansbury, Jr. 2003. Zeroing in on the pathogenic form of α-synuclein and its mechanism of neurotoxicity in Parkinson's disease. *Biochemistry.* 42:7871–7878.
27. Reixach, N. L., S. Deechongkit, …, J. N. Buxbaum. 2004. Tissue damage in the amyloidoses: transthyretin monomers and nonnative oligomers are the major cytotoxic species in tissue culture. *Proc. Natl. Acad. Sci. USA.* 101:2817–2822.
28. Serio, T. R., A. G. Cashikar, …, S. L. Lindquist. 2000. Nucleated conformational conversion and the replication of conformational information by a prion determinant. *Science*. 289:1317–1321.
29. Cheon, M., I. Chang, …, G. Favrin. 2007. Structural reorganisation and potential toxicity of oligomeric species formed during the assembly of amyloid fibrils. *PLOS Comput. Biol.* 3:1727–1738.
30. Lührs, T., C. Ritter, …, R. Riek. 2005. 3D structure of Alzheimer's amyloid-β (1-42) fibrils. *Proc. Natl. Acad. Sci. USA.* 102:17342–17347.
31. Petkova, A. T., Y. Ishii, …, R. Tycko. 2002. A structural model for Alzheimer's β-amyloid fibrils based on experimental constraints from solid state NMR. *Proc. Natl. Acad. Sci. USA.* 99:16742–16747.
32. Calamai, M., G. G. Tartaglia, …, C. M. Dobson. 2008. Mutational analysis of the aggregation-prone and disaggregation-prone regions of acylphosphatase. *J. Mol. Biol.* 387:965–974.
33. Wakutani, Y., K. Watanabe, …, K. Nakashima. 2004. Novel amyloid precursor protein gene missense mutation (D678N) in probable familial Alzheimer's disease. *J. Neurol. Neurosurg. Psychiatry.* 75:1039–1042.
34. Di Fede, G., M. Catania, …, F. Tagliavini. 2009. A recessive mutation in the APP gene with dominant-negative effect on amyloidogenesis. *Science.* 323:1473–1477.
35. Janssen, J. C., J. A. Beck, …, J. Collinge. 2003. Early onset familial Alzheimer's disease: mutation frequency in 31 families. *Neurology.* 60:235–239.
36. Uptain, S. M., and S. Lindquist. 2002. Prions as protein-based genetic elements. *Annu. Rev. Microbiol.* 56:703–741.
37. Fowler, D. M., A. V. Koulov, …, J. W. Kelly. 2006. Functional amyloid formation within mammalian tissue. *PLoS Biol.* 4:e6.
38. Chapman, M. R., L. S. Robinson, …, S. J. Hultgren. 2002. Role of *Escherichia coli* curli operons in directing amyloid fiber formation. *Science.* 295:851–855.